

Correlation and size dependence of the lattice strain, binding energy, elastic modulus, and thermal stability for Au and Ag nanostructures

X. J. Liu,¹ Z. F. Zhou,^{1,a)} L. W. Yang,¹ J. W. Li,¹ G. F. Xie,¹ S. Y. Fu,² and C. Q. Sun^{3,b)}

¹*Institute for Quantum Engineering and Micro-Nano Energy Technology, Key Laboratory of Low Dimensional Materials and Application Technology and Faculty of Materials, Optoelectronics and Physics, Xiangtan University, Hunan 411105, China*

²*Technical Institute of Physics and Chemistry, Chinese Academy of Sciences, Beijing 100080, China*

³*School of Electrical and Electronic Engineering, Nanyang Technological University, 639798 Singapore*

(Received 15 December 2010; accepted 7 February 2011; published online 12 April 2011)

As a group of wonder materials, gold and silver at the nanoscale demonstrate many intriguing properties that cannot be seen from their bulk counterparts. However, consistent insight into the mechanism behind the fascinations and their interdependence given by one integrated model is highly desirable. Based on Goldschmidt-Pauling's rule of bond contraction and its extension to the local bond energy, binding energy density, and atomic cohesive energy, we have developed such a model that is able to reconcile the observed size dependence of the lattice strain, core level shift, elastic modulus, and thermal stability of Au and Ag nanostructures from the perspective of skin-depth bond order loss. Theoretical reproduction of the measured size trends confirms that the undercoordination-induced local bond contraction, bond strength gain, and the associated binding energy density gain, the cohesive energy loss and the tunable fraction of such undercoordinated atoms dictate the observed fascinations, which should shed light on the understanding of the unusual behavior of other nanostructured materials as well. © 2011 American Institute of Physics. [doi:10.1063/1.3569743]

I. INTRODUCTION

Gold and silver at the nanoscale have demonstrated many intriguing chemical and physical properties that their bulk counterparts do not have. It is striking that all the detectable quantities such as the elastic modulus (Y), the melting point (T_m), and the energy shift (ΔE_v) of a certain v th core band keep no longer constant but they change linearly with the inverse of the feature size of the nanostructure. Experimental investigations and quantum simulations have revealed unexpectedly that the elastic modulus of Au and Ag at the nanoscale ascends^{1–5} by up to 100% and the melting point descends by 70%^{6–8} associated with a 50% positive shift of the core bands^{9–11} when the Au and Ag solids are reduced from the bulk to the atomic scale. The unusual performance of these nanostructures not only challenge for new knowledge but also have found applications in catalysis, photography, medicine, bio-image, information storage, surface enhanced Raman spectroscopy for single molecule detection and nano-interconnects in ultra-large-scale integration circuits, etc.^{12–17}

In order to understand the unusual behaviors of metallic nanostructures, numerous models have been developed from various perspectives. For the size-induced Y elevation, surface tension,^{18,19} surface relaxation,^{19,20} surface reconstruction,²¹ surface stress,^{1,22} bulk nonlinear elasticity,²³ and surface energy density gain²⁴ have been proposed; for the size-induced T_m depression, models such as liquid-shell nucleation and growth,²⁵ liquid-drop formation,⁶ lattice-

vibration instability,^{26,27} surface-phonon instability,²⁸ cohesive energy depression,²⁹ and surface bond-order imperfection³⁰ have been applied; for the size induced binding energy shift, models of “initial-final states” screening,³¹ core-hole surface relaxation,^{32,33} and “quantum entrapment”³⁴ have been proposed. Ao³³ proposed that the elastic modulus of Au and Cu change not only with particle size due to surface bond contraction but also with the temperate of operation. Although the models acknowledge the surface effect and surface energy, the origin of the unusual surface effect remains unclear. Is it possible to reconcile the size dependency using a single model with deeper insight into the physical origin of these observations?

Recent progress^{35,36} has shown that the size induced change of the quantities are interdependent and they arise from the same origin of atomic undercoordination. The shorter and stronger bonds in the surface skin up to two or three atomic layers dominate the size dependency while bonds in the core interior remain their bulk nature.²⁴ Taking Au and Ag nanostructures for example, this communication aims to emphasize that the bond order, bond length, bond energy, binding energy density and the cohesive energy per discrete atom in the surface skin originate while the surface-to-volume ratio determines the magnitude of the observed changes. Theoretical reconciliation of the observed size dependence of the lattice strain, elastic modulus, Y , melting point, T_m , and the core level shift for Ag and Au nanostructures can be realized by the concept of undercoordination, which not only confirms the theory expectations but also provides guidelines for nanoscale materials and device design.

^{a)}Electronic mail: zfzhou@xtu.edu.cn.

^{b)}Electronic mail: ecqsun@ntu.edu.sg.

II. PRINCIPLE

A. Physical origin: Atomic undercoordination

From the perspective of bond formation, dissociation, relaxation, and vibration and the associated dynamic and energetic behavior of charge polarization, repopulation, densification and localization, it has been derived that all the detectable quantities can be expressed as functional

dependence on the identities of bond order, z , bond nature, m , bond length, d_z , bond energy at equilibrium, E_z , of a representative bond for the entire specimen, and their derivatives of binding energy density, $E_d = E_z/d_z^3$ and atomic cohesive energy, $E_c = zE_z$, and the change of d_z and E_z under the applied stimulus such as pressure and temperature. At a specific atomic site, it can be derived,^{17,24,36}

$$\begin{cases} \varepsilon = 1 + C_z & (z\text{-induced strain}) \\ \Delta E_v \propto E_z \quad (eV) & (\text{Binding energy shift} \propto \text{bond energy at equilibrium}) \\ Y \propto E_z/d_z^3 \quad (eV/m^3) & (\text{Elastic modulus} \propto \text{energy density}) \\ T_m \propto zE_z \quad (eV/atom) & (\text{Melting point} \propto \text{atomic cohesive energy}) \end{cases}$$

with

$$\begin{cases} C_z = 2/\{1 + \exp[(12 - z)/(8z)]\} & (\text{Bond contraction coefficient}) \\ C_z^{-m} = E_z/E_b & (\text{Bond strengthening coefficient}). \end{cases} \quad (1)$$

The bond contraction coefficient C_z represents and duplicates the rule of Goldschmidt-Pauling bond contraction.³⁶ As a consequence of the spontaneous bond contraction, the bond energy increase from the bulk value of E_b to $E_z = C_z^{-m}E_b$ when the z is reduced from the bulk standard of 12 to z . The index m is the bond nature indicator that is not freely adjustable for a given material.

It is ready to derive the aforementioned relations as shown below. Given the Lenard-Jones potential $u(r)$, for instance, and taking the atoms as spheres with diameter or the equilibrium bond length (d), one can derive that the elastic modulus and the stress depend on the binding energy density at equilibrium and nonequilibrium conditions, respectively,²⁴

$$\begin{cases} P = -\frac{\partial u(r)}{\partial V} = -\frac{\partial u(r)}{\partial r} \frac{dr}{dV} \propto \frac{u(r)}{r^3} & (\text{Binding energy density at non-equilibrium}) \\ B = -V \frac{\partial^2 u(r)}{\partial V^2} \Big|_{r=d} = V \frac{\partial P}{\partial r} \frac{dr}{dV} \propto \frac{E_b}{d_b^3} & (\text{Binding energy density at equilibrium}). \end{cases} \quad (2)$$

The Young's modulus is $Y \sim 3B$. This formulation clarifies the atomistic origin and the correlation between the stress and the elastic modulus that have been a long confusion. The P and B describe different matters though they may be proportional to each other quantitatively and in the same dimension of Pa. The B is valid for elastic deformation at equilibrium and the P is for the plastic deformation at nonequilibrium. The derived expressions apply to any kind of interatomic potential as the modulus and the stress are related only to the bond length and bond energy.

Furthermore, the spontaneous bond contraction and bond strength gain lead to the local interatomic potential trap depression and energy densification, which can be detected using x-ray photoelectron spectroscopy as the energy shift of the v th core-level, $\Delta E_v(z) = E_v(z) - E_v(0)$, from that of an isolated atom, $E_v(0)$, which has been proven to be proportional to the cohesive energy per bond at equilibrium,⁹ The

energy shift of the z -coordinated atom is constrained by the relation,

$$\frac{\Delta E_v(z)}{\Delta E_v(12)} = \frac{E_v(z) - E_v(0)}{E_v(12) - E_v(0)} = \frac{E_z}{E_b} = C_z^{-m}, \quad (3)$$

where $\Delta E_v(12)$ is the bulk value. Likewise, one can imagine that evaporating a z -coordinated atom from a solid requires energy breaking all the bonds to its neighbors, i.e., the cohesive energy, zE_z . For the melting or other form of phase transition, the energy required per atom is only a certain portion of zE_z .

Therefore, all the discussed changes in Eq. (1) originate from the effect of undercoordination, $z < 12$, and its consequence on the bond length, bond strength, binding energy density, and atomic cohesive energy. The undercoordinated system also includes atomic vacancy, defect, surface, nanocavity, and grain boundary, etc.

B. The magnitudes of change: A core-shell configuration

Considering the fact that only bonds at the skin are shorter^{32,37-42} and stronger and contribute to the size effect while bonds in the core interior remain their bulk nature. Using a sum rule of the core-shell structure, we can derive the size dependency for a given quantity, Q ,

$$Q(K) = Q(\infty) + \sum_{i \leq 3} N_i(q_i - q_b)$$

with

$$Q(\infty) = Nq_b,$$

we have,

$$\begin{aligned} \Delta_Q &= \frac{Q(K) - Q(\infty)}{Q(\infty)} = \sum_{i \leq 3} \frac{N_i(q_i - q_b)}{Nq_b} \\ &= \sum_{i \leq 3} \gamma_i \left(\frac{\Delta q_i}{q_b} \right). \end{aligned} \quad (4)$$

Combining Eqs. (1) and (4), we have the following,

$$\begin{aligned} \Delta_Q &= \left\{ \begin{array}{l} \Delta_\varepsilon \\ \Delta_Y \\ \Delta_{T_m} \\ \Delta_{\Delta E_v} \end{array} \right\} \\ &= \sum_{i \leq 3} \gamma_i \left\{ \begin{array}{l} (C_i - 1) \quad (\text{Strain}) \\ (C_i^{-(m+3)} - 1) \quad (\text{Elastic modulus}) \\ (z_{ib} C_i^{-m} - 1) \quad (\text{Melting point}) \\ (C_i^{-m} - 1) \quad (\text{Core level shift}) \end{array} \right. \\ \gamma_i &= \frac{V_i}{V} = \frac{N_i}{N} = \frac{\tau C_i}{K} \quad (\text{Surface-to-volume ratio}). \end{aligned} \quad (5)$$

The surface-to-volume ratio of the i th atomic layer, γ_i , is counted up from $i=1$ to 3 from the outermost inward. The dimensionality $\tau = 1, 2$, and 3 correspond to a thin plate, a cylindrical rod and a spherical dot, respectively. The N_i and V_i correspond to the number and volume of the specific i th atomic layer of the nanostructure. The subscript i and b denotes the i th atomic layer and the bulk. K is the number of the atoms lined along the radius (R) of a nanosphere or a nanowire or across the thickness (R) of a thin film, and approximately equals to R/d_b . The q corresponds to the den-

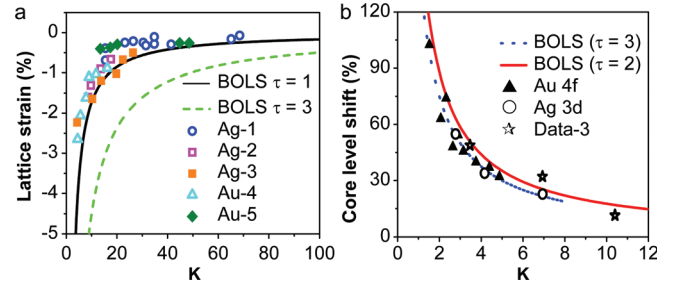


FIG. 1. (Color online) Theoretical reproduction of the size dependence of the (a) mean lattice strain of Ag and Au nanostructures with scattered data 1–5 being taken from Refs. 55–59 and (b) the Au-4f and Ag-3d core level shifts (binding energy) with data 1–3 taken from Refs. 10 and 11. The K on the X-axis is reduced size and equals approximately the number of atoms lined along the radius of a nanosphere or a nanowire or across the thickness of a thin film.

sity of Q . The effective CN of an atom in the specific i th atomic layer, z_i , varies with the curvature of a nanostructure in the form:³⁵ $z_1 = 4(1 - 0.75/K)$, $z_2 = z_1 + 2$ and $z_3 = 12$. The terms in the brackets of Eq. (5) originate and the γ_i determines the magnitude of the size induced change. The only key factor is the C_z . If $C_z = 1$, nothing will change. Therefore, the lattice strain, elastic modulus, melting point, and the core level shift as a whole are thus united with the extrinsic and intrinsic variables of $(\tau, K; z, m, d_z, E_z)$.

Generally, the measured size trends of $\varepsilon(K)$, $Y(K)$, $\Delta E_v(K)$ and $T_m(K)$ follow the linear dependence on the inverse size,

$$Q(K) = Q(\infty) \begin{cases} (1 + B_q K^{-1}) & (\text{Measurement}) \\ (1 + \Delta'_q \tau K^{-1}) & (\text{BOLS theory}). \end{cases} \quad (6)$$

Equaling the respective measurement with the BOLS formulation, we have $B_q = \tau \Delta'_q$ with $\Delta'_q = \Delta_q K / \tau$. We can obtain the bulk value of $Q(\infty)$ as the intercept of the measured $Q(K) \cdot K^{-1}$ plot.

III. RESULTS AND DISCUSSION

Ideally, the m is an intrinsic parameter that should not change for a given material; however, experimental artifacts such as surface passivation or the accuracy of size and dimensionality determination may lead to the m value to deviate. In order to optimize the m value for Ag example, we plotted the measured $\Delta Q(K)/Q(\infty)$ versus K^{-1} firstly to find the slope B_q with the known Ag-Ag bond length $d_0 = 0.289$ nm. An intercept offset was applied to ensure

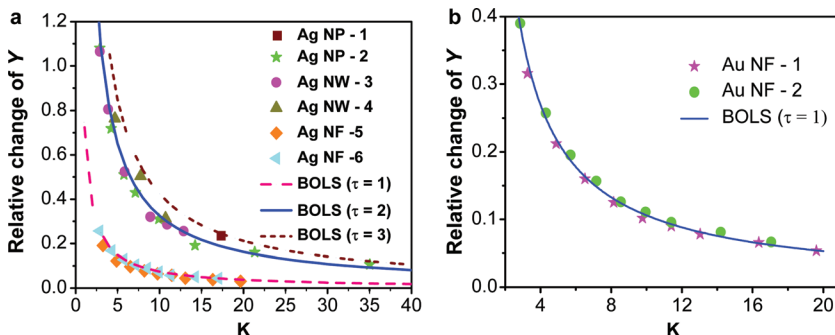


FIG. 2. (Color online) Theoretical reproduction of the size-enhanced elastic modulus (energy density) of (a) Ag nanostructures with the scattered Data 1–6 being taken from Refs. 2, 60, and 61 and (b) Au nanofilms with Data 1–2 from Ref. 61. The NF, NP, and NW represent for the nanofilm, particle, and wire.

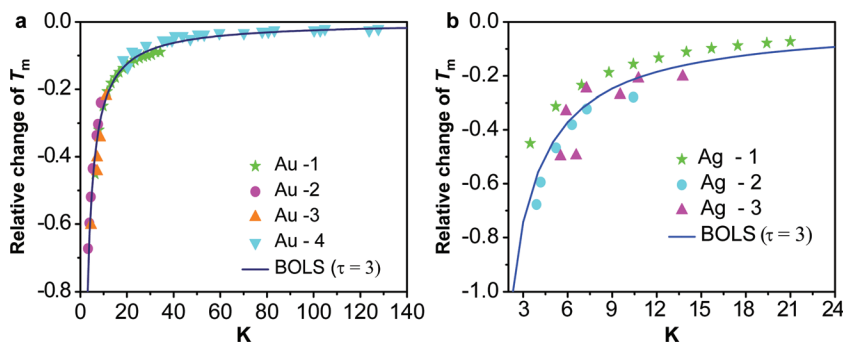


FIG. 3. (Color online) Theoretical reproduction of the size-depressed T_m (atomic cohesive energy) of (a) Ag nanostructures with Data 1–3 from Refs. 7, 62, and 63 and (b) Au nanoparticles with Data 1–4 from Refs. 64–67.

$\Delta Q(\infty)/Q(\infty) \equiv 0$. By using the relation of $B_q = \tau \Delta'_q$, we can calculate the values of Δ_q and determine the m value. The m values for Au and Ag were optimized to be 2.55 and 2.93, respectively, derived from the elastic modulus and melting point results in the ambient conditions. Under ultrahigh vacuum conditions, the $m = 1$ for many metals in general.³⁶

With the optimized m values we calculated and plotted the BOLS curves and then compared them with the measured data as shown in Figs. 1–3. Consistency between BOLS predictions and measurements has thus been realized. It is seen that the mean lattice strains and the mean melting points for both Au and Ag drop while the elastic modulus and the core level shifts rise monotonically with the inverse of size. These seemingly irrelevant quantities are thus uniquely unified with the BOLS premise. The reproduction of these quantities confirms the occurrences of bond relaxation and subsequent surface energy densification and atomic cohesive energy loss. In fact, the surface preferential straining of gold nanocrystals has been observed by many researchers.^{39–41} Using an electron cohesive diffraction, Huang *et al.*³⁹ discovered that the Au–Au bond contraction happens only to the outermost two interatomic spacing of a gold nanocrystal in a radial way while bonds in the core interior remain the bulk value, being consistent with molecular dynamics⁴³ and density functional theory³⁴ calculations and the current BOLS expectation. Recent measurements using the aberration-corrected imaging, the surface and terrace edge bonds have been measured to contract from Ag,⁴⁴ Pt,^{45–47} Co_3O_4 ,⁴⁸ substantially compared with the bulk values. The unification of these four seemingly irrelevant properties indicates that all the considered properties are correlated with the bond order, nature, length, and energy of the undercoordinated atoms in the surface up to skin depth.

It is well known that nanoparticles are usually polyhedral when their sizes become very small. Polyhedral particles exhibit surface energy and elastic anisotropy and different surfaces are decorated with different densities of unsaturated bonds. For instance, silver in particular has been shown to form in a variety of shapes, each with characteristic properties due to the atomic coordination change. This irregular shape-entity will affect the value of τ and z_i , as discussed. Recent XPS analysis⁴⁹ revealed that for the fcc (100), (110), and (111) surfaces of Pd and Rh, the z_1 values are 4.0, 3.75 and 4.25, respectively. The orientation-discriminated z_i values lead to slight modification of the surface bond energy and hence the considered quantities. Nevertheless, this kind

of geometric anisotropy only affects the accuracy of the τ values and has nothing to do with the nature, the origin, the trends and the interdependence of these quantities.

Another issue is the surface passivation. Coated with thiolated organic ligands, Au_{102} cluster demonstrates Au–Au bond expansion⁵⁰ arising from the diffusion of S atoms into the outermost atomic layer for Au–S bonding, being the same to oxygen chemisorption that causes Cu–Cu distance expansion but the O–Cu bond contracts in the surface skin.⁵¹ Very low-energy electron diffraction and scanning tunneling microscopy investigations revealed that oxygen atoms penetrate into the surface, which expands the first interlayer spacing from 0.180 nm to 0.194 nm but the Cu–O distances are 0.163, 0.174, and 0.194 nm in the Cu_3O_2 pairing tetrahedron. Chemisorption of electronegative atoms does alter the bond nature (m value) and bond length. Hence the surface passivation effect likely changes the surface energy, elasticity and melting point,⁵¹ as well. Excessive bulk defects would also lower the elasticity and melting point,^{52,53} like the metallic foams.⁵⁴ The defects serve as not only centers of failure but also sites of energy pinning. Under this condition, the strength of materials should be dominated by the competition between the structural failure and the energy pinning effect.

IV. CONCLUSION

In summary, from the perspective of bond order deficiency and its consequence on the bond length, bond strength, quantum trap, binding energy density and atomic cohesive energy in the surface skin, we have been able to reconcile the size dependence of the lattice strain, melting point depression, elastic enhancement and the core level shift of Ag and Au nanostructures with derived information of the core level binding energy of an isolated atom (see Table I).

TABLE I. Summary of the input and the derived information for Au and Ag nanostructures.

	Input				Output		
	d_b (nm)	Y_b (GPa)	T_m (K)	$E_v(12)$ (eV)	m	$E_v(0)$ (eV)	$\Delta E_v(12)$ (eV)
Ag	0.289	76	1235	368.3(3d)	2.93	367.431	0.869
Au	0.288	78.9	1337	84.37(4f)	2.55×1.0^9	81.504	2.866

Debating on the physical origins of the considered quantities and the paradox of the T_m depression and Y elevation due to size reduction has thus been clarified.

ACKNOWLEDGMENTS

Financial support from National NSF (Nos. 11002121 and 10802071) of China.

- ¹G. Y. Jing, H. L. Duan, X. M. Sun, Z. S. Zhang, J. Xu, Y. D. Li, J. X. Wang, and D. P. Yu, *Phys. Rev. B* **73**, 235409 (2006).
- ²M. T. McDowell, A. M. Leach, and K. Gaill, *Nano Lett.* **8**, 3613 (2008).
- ³Y. X. Chen, B. L. Dorgan, D. N. McLroy, and D. E. Aston, *J. Appl. Phys.* **100**, 104301 (2006).
- ⁴X. D. Li, H. S. Hao, C. J. Murphy, and K. K. Caswell, *Nano Lett.* **3**, 1495 (2003).
- ⁵B. Wu, A. Heidelberg, J. J. Boland, J. E. Sader, X. M. Sun, and Y. D. Li, *Nano Lett.* **6**, 468 (2006).
- ⁶K. K. Nanda, *Appl. Phys. Lett.* **87**, 021909 (2005).
- ⁷W. H. Luo, W. Y. Hu, and S. F. Xiao, *J. Chem. Phys. C* **112**, 2359 (2008).
- ⁸C. C. Yang and S. Li, *J. Chem. Phys. C* **112**, 16400 (2008).
- ⁹C. Q. Sun, *Phys. Rev. B* **69**, 045105 (2004).
- ¹⁰T. Ohgi and D. Fujita, *Phys. Rev. B* **66**, 115410 (2002).
- ¹¹I. Lopez-Salido, D. Lim, and Y. Kim, *Surf. Sci.* **588**, 6 (2005).
- ¹²N. F. Dummer, S. Bawaked, J. Hayward, R. Jenkins, and G. J. Hutchings, *Catal. Today* **154**, 2 (2010).
- ¹³Y. L. Wang, K. Lee, and J. Irudayaraj, *J. Chem. Phys. C* **114**, 16122 (2010).
- ¹⁴Y. Z. Xiang, Q. Q. Meng, X. N. Li, and J. G. Wang, *Chem. Comm.* **46**, 5918 (2010).
- ¹⁵Y. G. Sun and Y. N. Xia, *Science* **298**, 2176 (2002).
- ¹⁶J. Margueritat, J. Gonzalo, C. N. Afonso, A. Mlayah, D. B. Murray, and L. Saviot, *Nano Lett.* **6**, 2037 (2006).
- ¹⁷C. Q. Sun, *Nanoscale* **2**, 1930 (2010).
- ¹⁸S. Cuenot, C. Fretigny, S. Demoustier-Champagne, and B. Nysten, *Phys. Rev. B* **69**, 165410 (2004).
- ¹⁹J. G. Guo and Y. P. Zhao, *Nanotechnology* **18**, 295701 (2007).
- ²⁰T. Y. Zhang, M. Luo, and W. K. Chan, *J. Appl. Phys.* **103**, 104308 (2008).
- ²¹H. W. Shim, L. G. Zhou, H. C. Huang, and T. S. Cale, *Appl. Phys. Lett.* **86**, 151912 (2005).
- ²²G. Yun and H. S. Park, *Phys. Rev. B* **79**, 195421 (2009).
- ²³L. X. Zhang and H. C. Huang, *Appl. Phys. Lett.* **89**, 183111 (2006).
- ²⁴X. J. Liu, J. W. Li, Z. F. Zhou, L. W. Yang, Z. S. Ma, G. F. Xie, Y. Pan, and C. Q. Sun, *Appl. Phys. Lett.* **94**, 131902 (2009).
- ²⁵R. R. Vanfleet and J. M. Mochel, *Surf. Sci.* **341**, 40 (1995).
- ²⁶F. G. Shi, *J. Mater. Res.* **9**, 1307 (1994).
- ²⁷Q. Jiang and C. C. Yang, *Current Nanosci.* **4**, 179 (2008).
- ²⁸M. Wautelet, *J. Phys. D Appl. Phys.* **24**, 343 (1991).
- ²⁹W. Liu, D. Liu, W. T. Zheng, and Q. Jiang, *J. Chem. Phys. C* **112**, 18840 (2008).
- ³⁰G. Guisbiers, M. Kazan, O. Van Overschelde, M. Wautelet, and S. Pereira, *J. Chem. Phys. C* **112**, 4097 (2008).
- ³¹M. Alden, H. L. Skriver, and B. Johansson, *Phys. Rev. Lett.* **71**, 2457 (1993).
- ³²B. S. Fang, W. S. Lo, T. S. Chien, T. C. Leung, C. Y. Lue, C. T. Chan, and K. M. Ho, *Phys. Rev. B* **50**, 11093 (1994).
- ³³Z. M. Ao, S. Li, and Q. Jiang, *Appl. Phys. Lett.* **93**, 081905 (2008).
- ³⁴X. Zhang, J. L. Kuo, M. X. Gu, F. X. F. P. Bai, Q. G. Song, and C. Q. Sun, *Nanoscale* **2**, 412 (2010).
- ³⁵C. Q. Sun, *Prog. Mater. Sci.* **54**, 179 (2009).
- ³⁶C. Q. Sun, *Prog. Solid State Chem.* **35**, 1 (2007).
- ³⁷D. M. Riffe and G. K. Wertheim, *Phys. Rev. B* **47**, 6672 (1993).
- ³⁸N. Wu, Y. B. Losovyj, Z. Yu, R. F. Sabirianov, W. N. Mei, N. Lozova, J. A. C. Santana, and P. A. Dowben, *J. Phys. Condens. Matter.* **21**, 474222 (2009).
- ³⁹W. J. Huang, R. Sun, J. Tao, L. D. Menard, R. G. Nuzzo, and J. M. Zuo, *Nat. Mater.* **7**, 308 (2008).
- ⁴⁰J. T. Miller, A. J. Kropf, Y. Zha, J. R. Regalbuto, L. Delannoy, C. Louis, E. Bus, and J. A. van Bokhoven, *J. Catal.* **240**, 222 (2006).
- ⁴¹V. Petkov, Y. Peng, G. Williams, B. H. Huang, D. Tomalia, and Y. Ren, *Phys. Rev. B* **72**, 195402 (2005).
- ⁴²D. Q. Yang and E. Sacher, *Appl. Surf. Sci.* **195**, 187 (2002).
- ⁴³W. H. Qi, B. Y. Huang, and M. P. Wang, *J. Comput. Theor. Nanosci.* **6**, 635 (2009).
- ⁴⁴D. S. Su, T. Jacob, T. W. Hansen, D. Wang, R. Schlögl, B. Freitag, and S. Kujawa, *Angew. Chem. Int. Ed.* **47**, 5005 (2008).
- ⁴⁵S. W. Lee, S. Chen, J. Suntivich, K. Sasaki, R. R. Adzic, and Y. Shao-Horn, *J. Phys. Chem. Lett.* **1**, 1316 (2010).
- ⁴⁶L. C. Gontard, L.-Y. Chang, C. J. D. Hetherington, A. I. Kirkland, D. Ozkaya, and R. E. Dunin-Borkowski, *Angew. Chem. Int. Ed.* **46**, 3683 (2007).
- ⁴⁷N. Shibata, A. Goto, S. Y. Choi, T. Mizoguchi, S. D. Findlay, T. Yamamoto, and Y. Ikuhara, *Science* **322**, 570 (2008).
- ⁴⁸R. Yu, L. H. Hu, Z. Y. Cheng, Y. D. Li, H. Q. Ye, and J. Zhu, *Phys. Rev. Lett.* **105**, 226101 (2010).
- ⁴⁹Y. Wang, Y. G. Nie, J. S. Pan, L. K. Pan, Z. Sun, L. L. Wang, and C. Q. Sun, *Phys. Chem. Chem. Phys.* **12**, 2177 (2010).
- ⁵⁰P. D. Jadzinsky, G. Calero, C. J. Ackerson, D. A. Bushnell, and R. D. Kornberg, *Science* **318**, 430 (2007).
- ⁵¹C. Q. Sun, *Prog. Mater. Sci.* **48**, 521 (2003).
- ⁵²Q. S. Mei and K. Lu, *Prog. Mater. Sci.* **52**, 1175 (2007).
- ⁵³V. P. Adiga, A. V. Sumant, S. Suresh, C. Gudeman, O. Auciello, J. A. Carlisle, and R. W. Carpick, *Phys. Rev. B* **79**, 245403 (2009).
- ⁵⁴Y. Ding, C. Q. Sun, and Y. C. Zhou, *J. Appl. Phys.* **103**, 084317 (2008).
- ⁵⁵H. J. Wasserma and J. S. Vermaak, *Surf. Sci.* **22**, 164 (1970).
- ⁵⁶A. Kara and T. S. Rahman, *Phys. Rev. Lett.* **81**, 1453 (1998).
- ⁵⁷P. A. Montano, W. Schulze, B. Tesche, G. K. Shenoy, and T. I. Morrison, *Phys. Rev. B* **30**, 672 (1984).
- ⁵⁸D. Buttard, G. Dolino, C. Faivre, A. Halimaoui, F. Comin, V. Formoso, and L. Ortega, *J. Appl. Phys.* **85**, 7105 (1999).
- ⁵⁹H. Müller, C. Opitz, K. Strickert and L. Z. Skala, *Z. Phys. Chem. (Leipzig)* **268**, 634 (1987).
- ⁶⁰Q. F. Gu, G. Krauss, W. Steurer, F. Gramm, and A. Cervellino, *Phys. Rev. Lett.* **100**, 045502 (2008).
- ⁶¹F. H. Streitz, R. C. Cammarata, and K. Sieradzki, *Phys. Rev. B* **49**, 10699 (1994).
- ⁶²T. Castro, R. Reifengerger, E. Choi, and R. P. Andres, *Phys. Rev. B* **42**, 8548 (1990).
- ⁶³S. J. Zhao, S. Q. Wang, D. Y. Cheng, and H. Q. Ye, *J. Phys. Chem. B* **105**, 12857 (2001).
- ⁶⁴S. Arcidiacono, N. R. Bieri, D. Poulidakos, and C. P. Grigoropoulos, *Int. J. Multiphase Flow* **30**, 979 (2004).
- ⁶⁵J. R. Sambles, *Proc. R. Soc. London Ser. A* **324**, 339 (1971).
- ⁶⁶G. Schmidt and K. J. Klabunde (Wiley, New York, 2001), pp. 23.
- ⁶⁷F. Celestini, R. J. M. Pellenq, P. Bordarier, and B. Rousseau, *Z. Phys. D* **37**, 49 (1996).